Tailoring Biomass-Derived Carbon for High-Performance Supercapacitor from Controllably Cultivated Algae Microspheres

Bingjun Zhu [a†], Bin Liu [b,c†], Chong Qu [a†], Hao Zhang [a], Wenhan Guo [a], Zibin Liang [a], Feng Chen [b,c*], Ruqiang Zou [a*]

[a] *Beijing Key Laboratory for Theory and Technology of Advanced Battery Materials, Department of Materials Science and Engineering, College of Engineering, Peking University, Beijing 100871, P. R. China. Email: rzou@pku.edu.cn*

[b] *Institute for Food & Bioresource Engineering, College of Engineering, Peking University, Beijing 100871, China. Email: sfchencoe@pku.edu.cn*

[c] *BIC-ESAT, College of Engineering, Peking University, Beijing 100871, China*

[†] *The authors share equal contribution to this work*

1. Nutrients in cultivation medium

Besides KNO_3 and NaH_2PO_4•H_2O, the Kuhl medium consisted (per liter) of 30 g glucose, 0.247 g $MgSO_4$•$7H_2O$, 14.7 mg $CaCl_2$•$2H_2O$, 6.95 mg $FeSO_4$•$7H_2O$, 0.061 mg H_3BO_3, 0.169 mg $MnSO_4$•H_2O, 0.287 mg $ZnSO_4$•$7H_2O$, 0.0025 mg $CuSO_4$•$5H_2O$, and 0.01235 mg $(NH_4)_6MO_7O_{24}$•$4H_2O$. The BG11 medium consisted (per liter) of 1 mg Na_2 EDTA, 36 mg $CaCl_2 \cdot 2H_2O$, 75 mg $MgSO_4 \cdot 7H_2O$, 40 mg $K_2HPO_4 \cdot 3H_2O$, 2.86 mg H_3BO_3, 1.81 mg $MnCl_2 \cdot 4H_2O$, 0.222 mg $ZnSO_4 \cdot 7H_2O$, 0.079 mg $CuSO_4 \cdot 5H_2O$, 0.05 mg $CoCl_2 \cdot 6H_2O$, 0.391 mg $NaMoO_4 \cdot 2H_2O$ and 1500 mg $NaNO_3$.

2. Characterization of components in algae

The lipid content was determined by the Bligh method. In brief, lipids were extracted from lyophilized algal cells in a chloroform-methanol-water (4:2:1.5, by volume) system. The chloroform layer was evaporated under nitrogen gas to a constant weight.

For the determination of protein content, 10 mg lyophilized algal biomass was hydrolyzed in 200 μL 1 M NaOH and then incubated in a water bath at 80 °C for 10 min. Then, the hydrolysate volume was adjusted to 2 mL by H_2O and centrifuged at 12,000 g for 30 min. Next, the protein concentration of the supernatant was measured by the Protein assay kit (Bio-Rad #5000002, Hercules, USA) with bovine serum albumin as the standard.

Carbohydrate content was determined by the method previously published by Ma et al.. Briefly, lyophilized algal biomass was suspended in trifluoroacetic acid and then boiled for 4 h to release reducing sugars. Then, 20 μL supernatant was mixed with sulfuric acid (98 wt.%):water:phenol (300:150:3, v/v/w) and boiled for 20 min prior to reading the optical density at 490 nm. Glucose was used to establish the standard curve for the quantification of total carbohydrate content.

3. Galvanostatic charge-discharge measurement calculation

The specific capacitance was calculated from the galvanostatic charge-discharge measurements using the following equation,

$$C = \frac{2i_m \int V dt}{V^2 \Big|_{V_i}^{V_f}} \qquad \text{Equation S1}$$

C represents the galvanostatic charge-discharge (GCD) specific capacitance. $\int V dt$ is the integral current area, where V is the potential with initial and final values of V_i and V_f, respectively. $i_m = I/m$ is the current density, where I is the current and m is the mass of active materials.

4. SEM images of algae-derived carbon

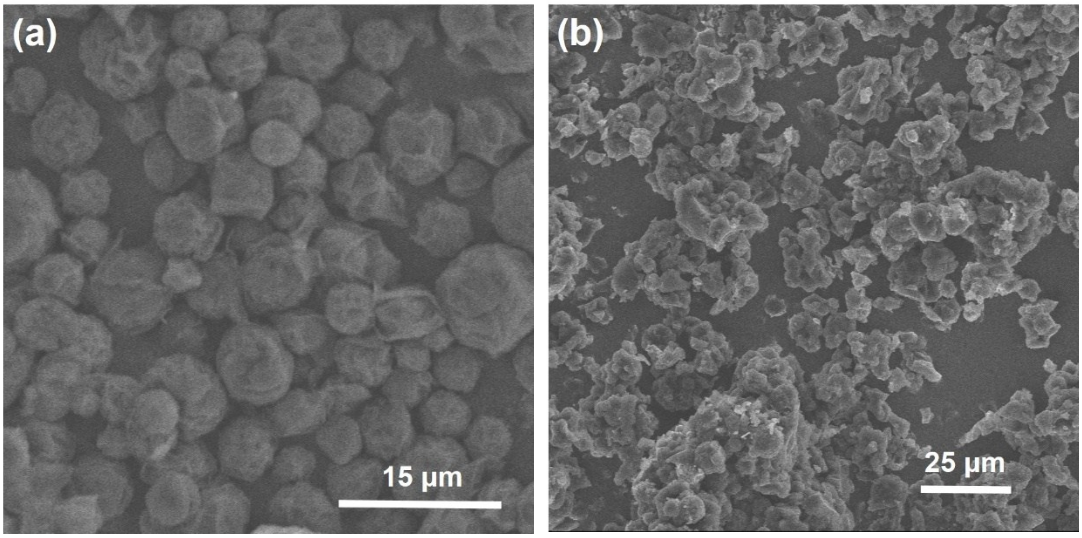

Figure S1: Lower magnification SEM images of original algae and activated algae-derived carbon.

5. High-resolution Na 1s XPS spectrum of AC3

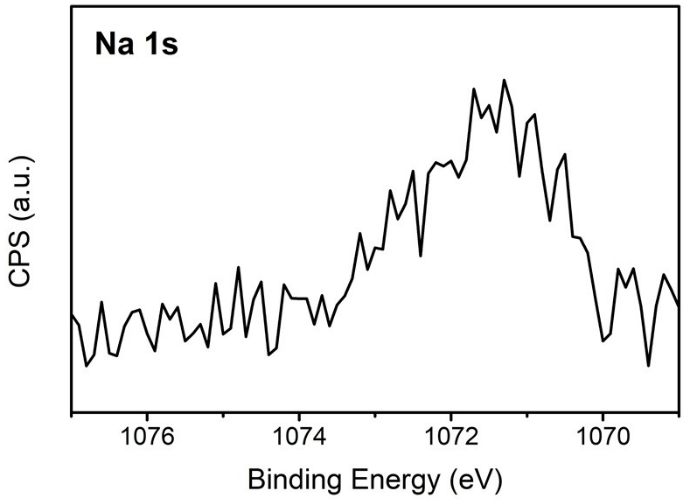

Figure S2: High-resolution Na 1s XPS spectrum of the algae-derived carbon AC3.

6. Capacitive performance of AC1

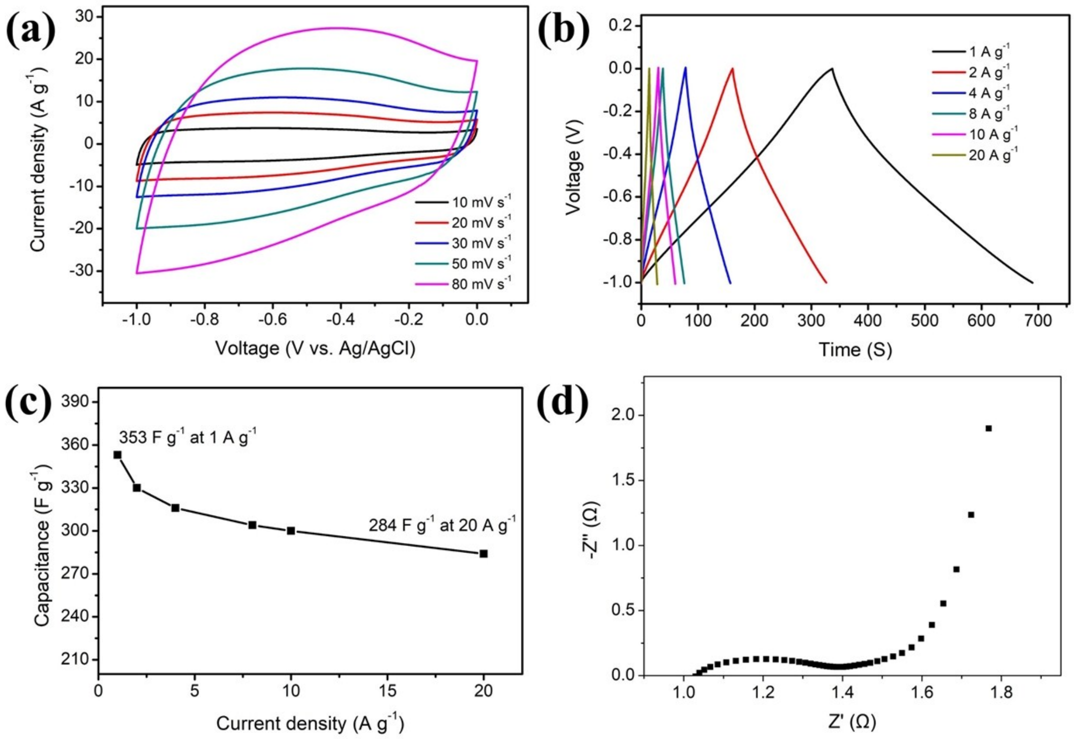

Figure S3: Capacitive performance of algae-derived carbon AC2: (a) CV curves at different scan rates. (b) GCD curves at different current densities. (c) Specific capacitance showing specific capacitance of 353, 316, 304, 300 and 284 F g^{-1} at the current density of 1, 2, 4, 8, 10 and 20 A g^{-1}. (d) Nyquist plot.

7. **Capacitive performance of AC2**

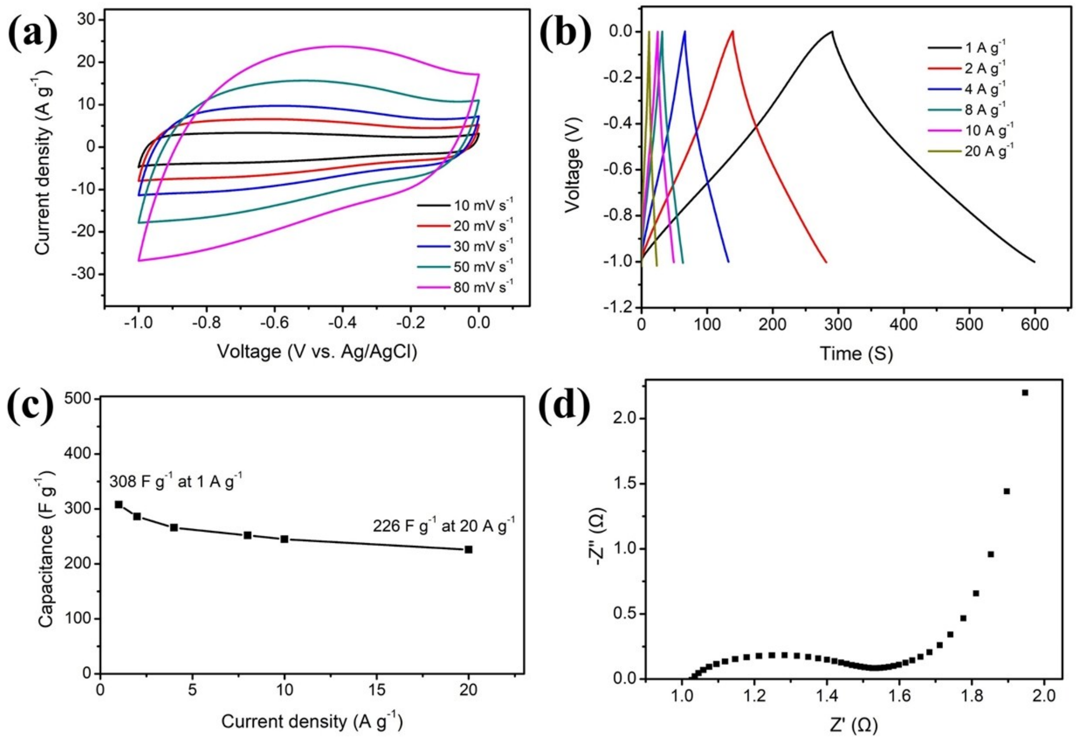

Figure S4: Capacitive performance of algae-derived carbon AC2: (a) CV curves at different scan rates. (b) GCD curves at different current densities. (c) Specific capacitance showing specific capacitance of 308, 286, 266, 252, 245, 226 F g^{-1} at the current density of 1, 2, 4, 8, 10 and 20 A g^{-1}. (d) Nyquist plot.

8. Capacitive performance of AC3

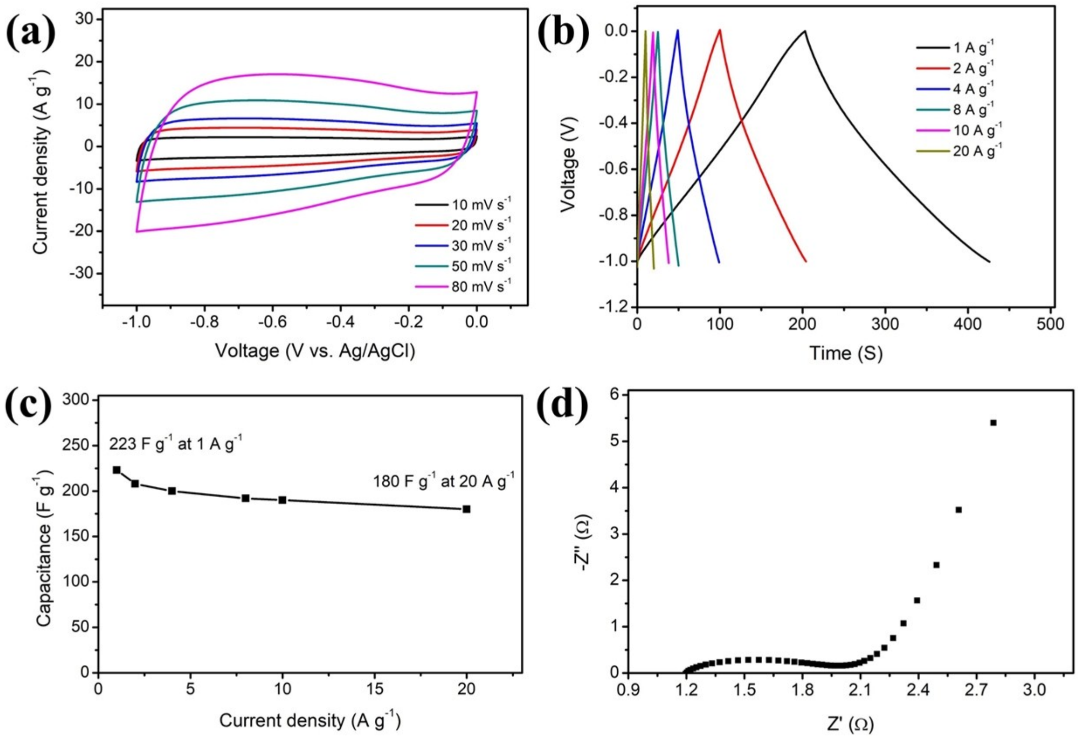

Figure S5: Capacitive performance of algae-derived carbon AC3: (a) CV curves at different scan rates. (b) GCD curves with at different current densities. (c) Specific capacitance showing specific capacitance of 223, 208, 200, 192, 190 and 180 F g^{-1} at the current density of 1, 2, 4, 8, 10 and 20 A g^{-1}. (d) Nyquist plot.

9. Capacitive performance of AC4

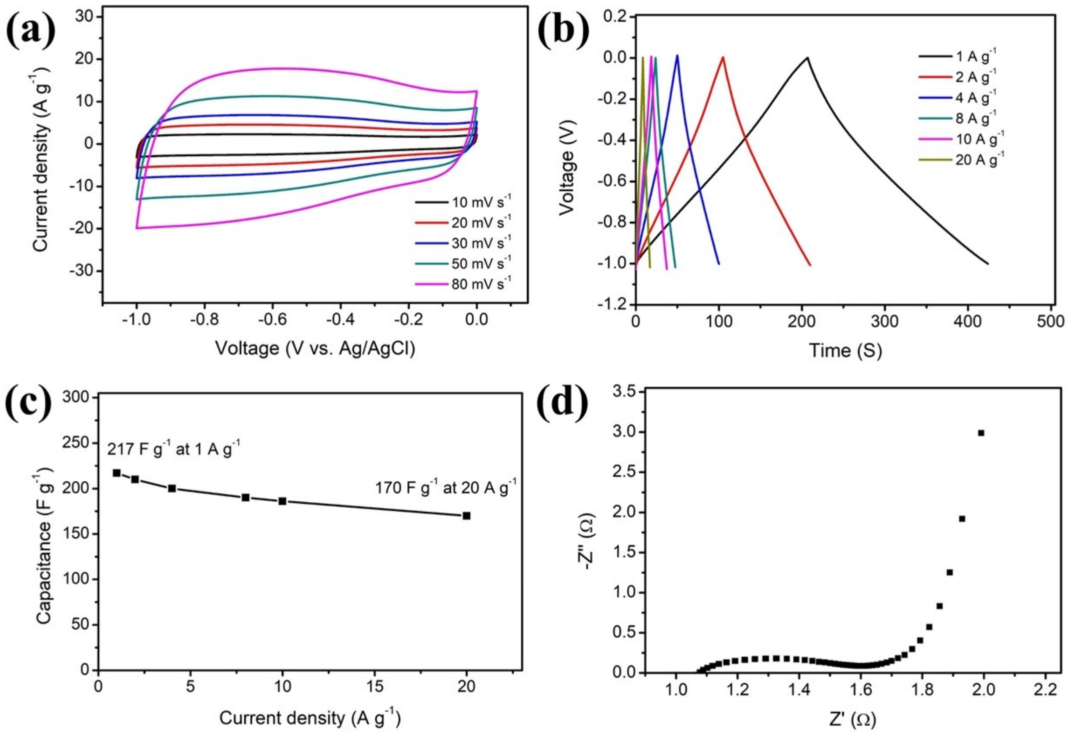

Figure S6: Capacitive performance of algae-derived carbon AC4: (a) CV curves at different scan rates. (b) GCD curves with at different current densities. (c) Specific capacitance showing specific capacitance of 217, 210, 200, 190, 186, 170 F g^{-1} at the current density of 1, 2, 4, 8, 10 and 20 A g^{-1}. (d) Nyquist plot.

10. Pore size distribution of AC1 and AC2

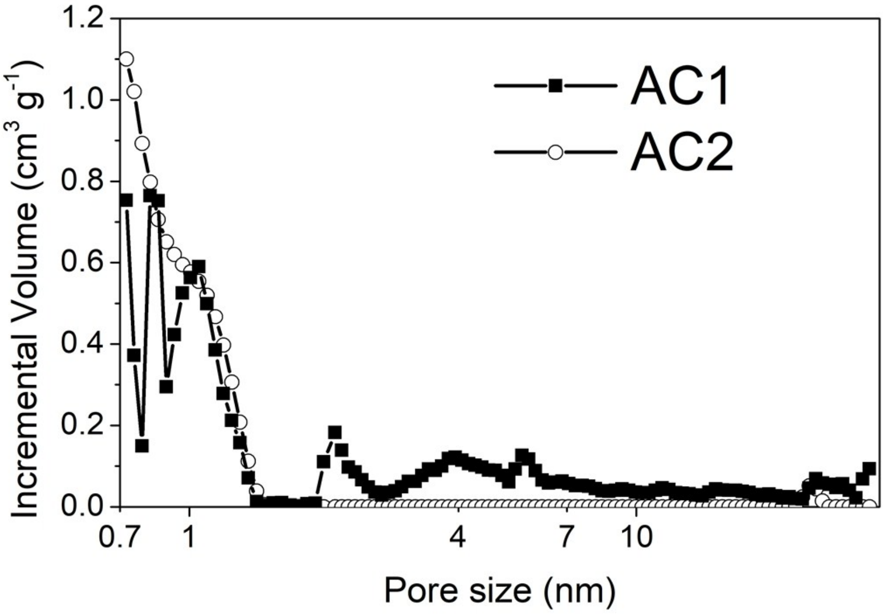

Figure S7: Pore size distribution of AC1 and AC2, showing AC2, showing AC2 mainly possesses pores less than 1.5 nm, while AC2 exhibits meospore size distribution above 2 nm.

11. Experimental information for specific energy density and power density calculation

The electrochemical measurements of the symmetric two-electrode device with MPF30AC-100 separator (Nippon Kodoshi Corporation, Kochi, Japan) and carbon fiber paper (CFP) current collector in a split test cell (MTI Corporation) configuration were carried out in a 2 M KOH electrolyte. The CV curves of the AC1//AC1 symmetric device were acquired in a potential range between 0 and 1 V at different scan rates, and the charge-discharge processes were performed by cycling the potential from 0 to 1 V at different current densities.

The energy density E (Wh kg^{-1}) and power density P (W kg^{-1}) in Ragone plot were calculated with the following equations,

$$E = \frac{1}{2} \cdot \frac{C \cdot \Delta V^2}{3.6} \qquad \text{Equation } S2$$

$$P = 3600 \cdot \frac{E}{\Delta t} \qquad \text{Equation } S3$$

Where C is the specific gravimetric capacitance of the device (F g^{-1}), ΔV is the potential window (V), and Δt is the discharge time (S).

12. Fabrication of two-electrode symmetric device

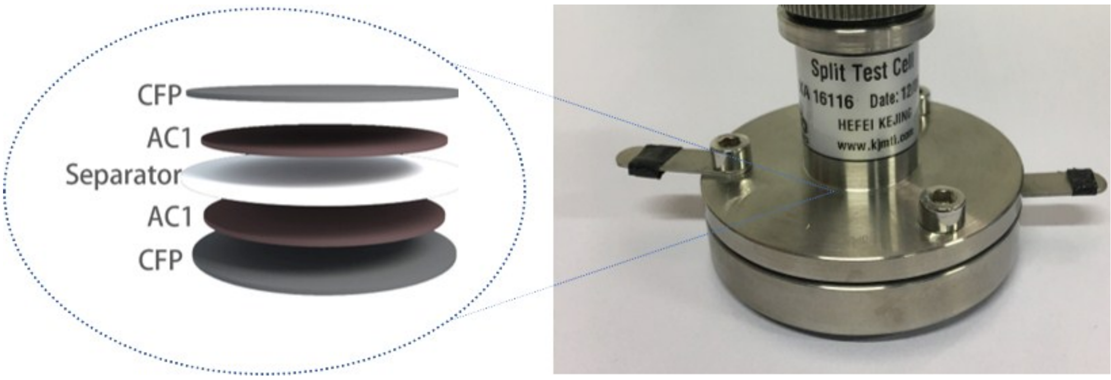

Figure S8: An illustration of the two-electrode symmetric device fabricated by using two identical AC1 electrodes.

13. Capacitive performance of the AC1//AC1 symmetric device

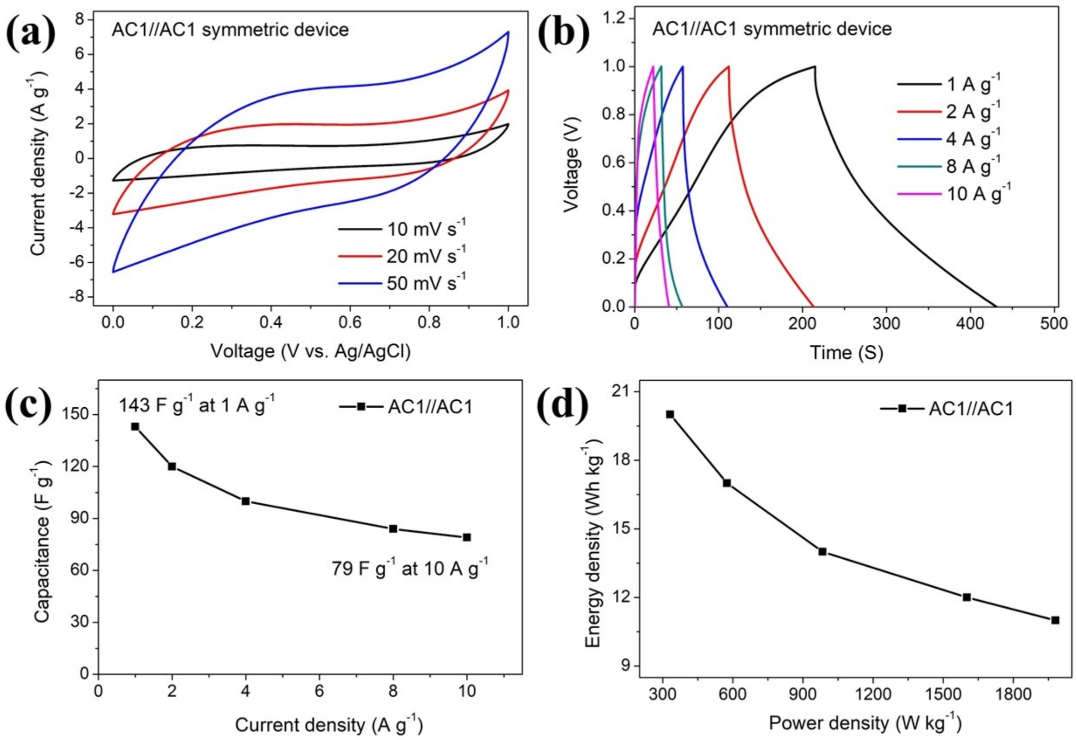

Figure S9: Capacitive performance of two-electrode symmetric device AC1//AC1: (a) CV curves at different scan rates. (b) GCD curves with at different current densities. (c) Specific capacitance showing specific capacitance of 143, 120, 100, 84 and 79 F g^{-1} at the current density of 1, 2, 4, 8, 10 and 20 A g^{-1}. (d) Ragone plot demonstrates a high energy density of 20 Wh kg^{-1} at the power density of 332 W kg^{-1} and retained 11 Wh kg^{-1} at elevated working power of 1980 W kg^{-1}.

14. Comparison of algae microstructures

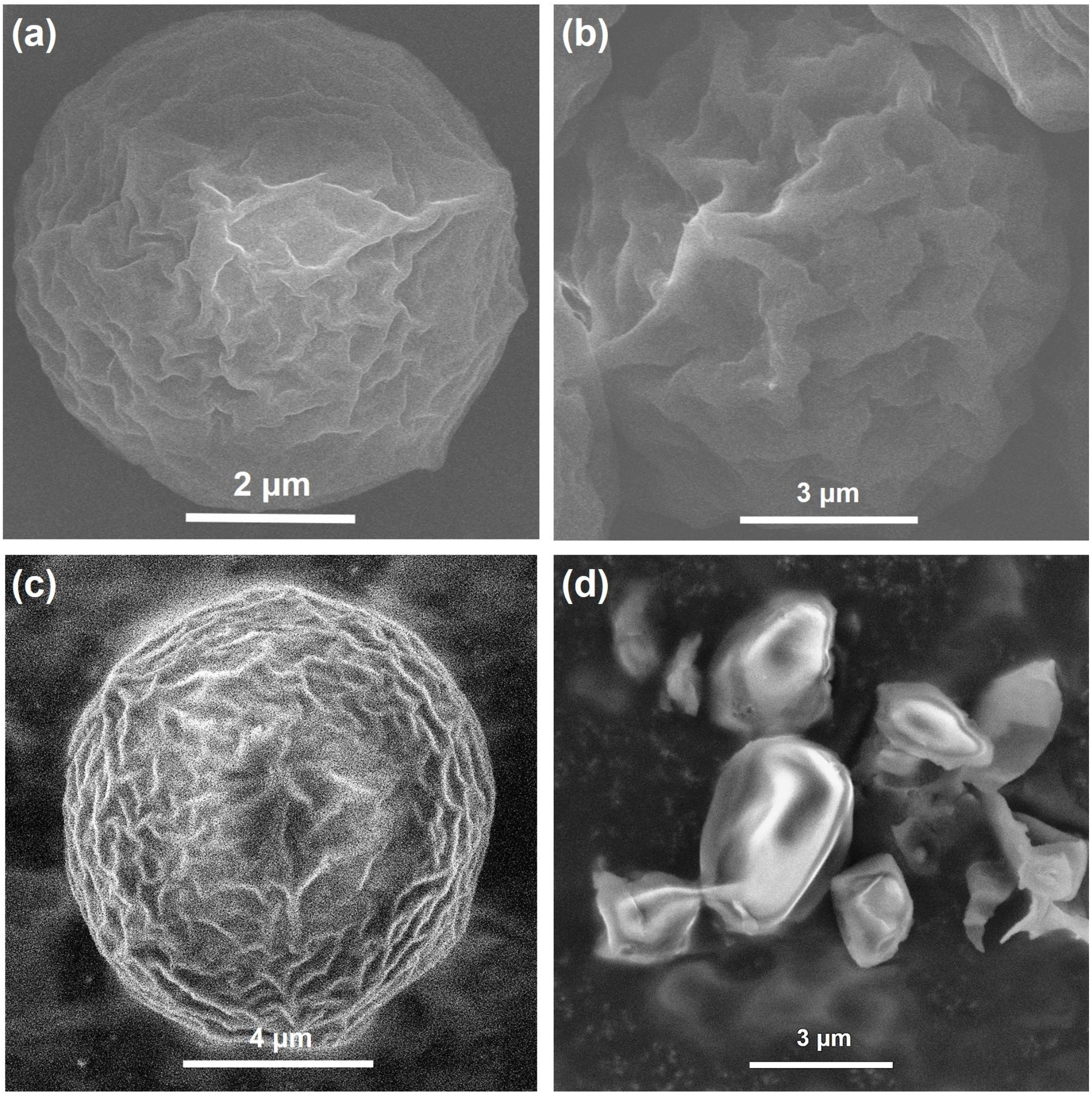

Figure S10: The SEM images (a), (b) and (c) demomstrate that Alga A1, A2 and A3 possess similar shapes and sizes. The algae sample A4 is cultivated based on a different algae strain. Therefore, its shape and size are different from those of the former three.